Evidence for superthermal secondary electrons produced by SEP ionization in the Martian atmosphere

Robert J. Lillis,[1] David A. Brain,[2] Gregory T. Delory,[1] David L. Mitchell,[1] Janet G. Luhmann,[1] and Robert P. Lin[1,3]

Received 15 August 2011; revised 21 November 2011; accepted 20 December 2011; published 8 March 2012.

[1] The atmosphere of Mars, lacking a global magnetic field, is exposed to the precipitation of solar energetic particles (SEPs), resulting in impact ionization and the production of secondary electrons, some of which may escape the atmosphere. In this study, we examine upward traveling fluxes of superthermal electrons between ~100 and 650 eV, measured by the Mars Global Surveyor Magnetometer/Electron Reflectometer at 400 km altitude during nine of the largest and clearest SEP events of the last solar maximum from November 2000 until the "Halloween" storms of late 2003. We subtract the contribution from backscattered low-energy precipitating electrons and find that, for the highest and most rarely observed SEP fluxes, we detect a statistically significant flux of SEP-produced superthermal electrons escaping the Martian atmosphere. The measured fluxes are found to be in broad agreement with a calculation of expected upward electron fluxes resulting from ionization of neutrals by energetic proton impact. Peak SEP ionization rates on the nightside from the Halloween storms are found to be comparable to (although lower than) typical dayside photoionization rates and at least 3 orders of magnitude higher than average nightside electron impact ionization rates. Further advances in our knowledge of SEP effects on the Martian ionosphere await data from the Radiation Assessment Detector (RAD) instrument on the Mars Science Laboratory rover in 2012 and the MAVEN orbiter in 2014.

Citation: Lillis, R. J., D. A. Brain, G. T. Delory, D. L. Mitchell, J. G. Luhmann, and R. P. Lin (2012), Evidence for superthermal secondary electrons produced by SEP ionization in the Martian atmosphere, *J. Geophys. Res.*, *117*, E03004, doi:10.1029/2011JE003932.

1. Introduction

[2] SEP (solar energetic particle) ions precipitating into the terrestrial atmosphere have for several decades been known to cause substantial ionization and other changes in the neutral atmosphere. Such precipitation, primarily protons, typically happens in the magnetic polar regions because of the shielding effects of closed magnetic field lines at lower geomagnetic latitudes [e.g., *Velinov*, 1968]. Past studies have utilized Monte Carlo modeling [e.g., *Velinov et al.*, 1996] and simultaneous spacecraft measurements of precipitating SEP spectra, in situ sounding rocket measurements of ion densities, and ground-based ionospheric radar data [e.g., *Reagan and Watt*, 1976] in order to characterize the resulting effects on plasma densities and neutral and plasma temperatures. Energy deposition from so-called polar cap absorption (PCA) events have been observed to cause substantial increases in plasma density (both electrons and ions) and nitric oxide concentration, ozone depletion, and decreases in water cluster ions [*Mitra and Rowe*, 1974; *Solomon et al.*, 1983; *Zadorozhnyi et al.*, 1992; *Jackman et al.*, 2008; *Seppälä et al.*, 2008]. Such efforts have led to a reasonably solid, if not complete, understanding of SEP-induced chemistry changes, heating, and ionization, in the terrestrial atmosphere [e.g., *Chevalier et al.*, 2007; *Dmitriev and Yeh*, 2008].

[3] However, although secondary electrons from proton aurora have been considered in some depth [e.g., *Lummerzheim et al.*, 2003; *Galand et al.*, 2002], not much work has been done on the secondary electron signatures specifically from solar proton events. Yet these particles carry possibly important information about both the incident spectrum and flux and its effects on the atmosphere.

[4] The role of a significant planetary magnetic field as a "shield" for a terrestrial planet's atmosphere and surface has long been debated [e.g., *Moore and Horwitz*, 2007]. In addition to atmospheric erosion by the solar wind, space weather events are expected to have distinctive effects on weakly magnetized bodies, including heating, ionization, dissociation, excitation, charge exchange, and (for energies

[1]Space Sciences Laboratory, University of California Berkeley, Berkeley, California, USA.
[2]Laboratory for Atmospheric and Space Physics, University of Colorado, Boulder, Colorado, USA.
[3]School of Space Research, Kyung Hee University, Yongin, Gyeonggi, South Korea.

0148-0227/12/2011JE003932

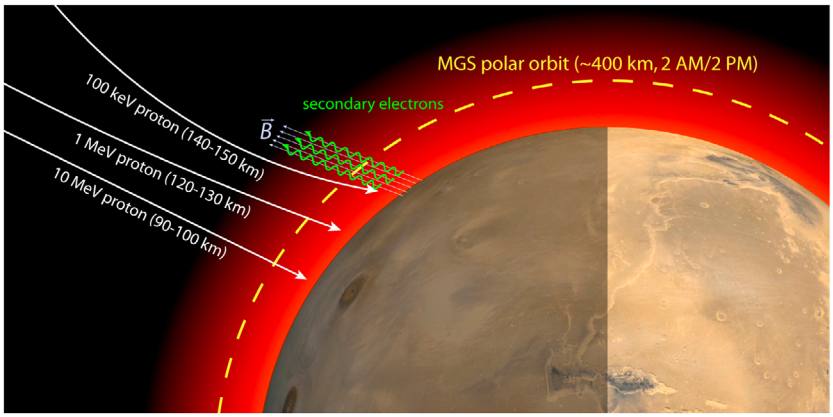

Figure 1. Illustration showing incident SEP protons of three different energies and the altitudes at which they deposit most of their energy, as well as the SEP-produced secondary electron's helical paths. Both intersect the MGS orbit. The proton gyroradii and MGS orbit are approximately accurate relative to the planet, whereas the electrons' gyroradii are greatly exaggerated so as to be visible.

above a few MeV) nuclear excitation from the near-total access of solar energetic particles to the atmosphere. Mars represents a particularly interesting case because of its potential for having had a previously habitable climate [e.g., *Bibring et al.*, 2006] wherein SEPs and their episodic and time-integrated effects on the atmosphere and surface should be considered integral parts of the Mars climate system.

[5] The information on SEP effects on the Martian atmosphere and surface is limited by lack of specific observations. We are thus left to infer their impacts from indirect measurements and models. SEPs below ~50 keV are typically appreciably deflected by the induced magnetosphere [*Leblanc et al.*, 2002], while those above ~50 keV can reach the collisional atmosphere and precipitate. SEP ions will always precipitate all over the side of the planet penetrated by the projected interplanetary magnetic field path (typically at ~57° to the Mars-Sun line assuming a Parker spiral) to the SEP source (i.e., a solar flare or interplanetary shock) [*Luhmann et al.*, 2007]. Depending on the pitch angle anisotropy of the particular event [*Reames et al.*, 2001], because of their typically very large gyroradii, SEPs may also often precipitate over the rest of the planet.

[6] Compared with the terrestrial case, measurements of SEP effects at Mars are scarce. We have evidence of SEP-produced ionization in the Martian atmosphere from observations of radar wave absorption and distortion in the dayside ionosphere by the MARSIS instrument on Mars Express. Radar reflections from the Martian surface were seen to disappear [*Morgan et al.*, 2006; *Espley et al.*, 2007] and derived total electron content was seen to increase [*Lillis et al.*, 2010] at times of SEP events. In addition, rates of heavy ion outflow from the Martian atmosphere increased approximately 1 order of magnitude during a particularly intense SEP event in December 2006 [*Futaana et al.*, 2008].

[7] In this paper, we attempt to gain further quantitative insight into the ionizing effects of SEPs in the Martian atmosphere by examining superthermal, presumably secondary, electrons of ionospheric origin observed traveling upward out of Mars' ionosphere during SEP events. Figure 1 is an illustration of the situation we examine whereby SEP ions collide with atmospheric neutrals, ionizing them and producing secondary electrons, some of which then escape the atmosphere, following helical paths around the local magnetic field. These are shown on the Martian nightside, where the all the analyzed data are collected (see section 3). The magnetic field shown is a typical nightside magnetotail field direction in the northern hemisphere away from strong crustal fields [e.g., *Ferguson et al.*, 2005].

2. Data

[8] We consider two different data products from the Magnetometer/Electron Reflectometer (MAG/ER) instrument [*Mitchell et al.*, 2001] onboard the Mars Global Surveyor (MGS) spacecraft, collected during the mapping phase of the mission from May 1999 until November 2006 when MGS was in an almost-circular 370 km × 430 km orbit [*Albee et al.*, 2001]. The first data set is pitch angle distributions (PADs) of superthermal solar wind electrons (pitch angle is the angle between electron velocity and magnetic field direction) at superthermal energies ranging from 100 to 650 eV. The second data set is the count rate from the highest-energy channel (16–20 keV) of the Electron Reflectometer instrument. Counts seen in this channel can come from either "real" 16–20 keV electrons that pass through the optics of the MAG/ER instrument or from energetic ions (>~30 MeV) that penetrate the aluminum housing of the instrument and interact directly with the microchannel plates (MCPs), causing equal numbers of counts in all energy channels. The effective geometric factor for real electrons is 0.02 cm^2 sr while for the penetrating particles it is roughly 3 orders of magnitude higher, of the order of $0.8\pi A$ = ~40 cm^2 sr, where A is the area of the MCP and 0.8 accounts for shadowing by the body of Mars. These penetrating particle counts are from two sources: galactic cosmic rays (GCRs) and SEP ions (mostly protons). GCRs cause on average 5–15 counts per second, varying quite slowly over the mission lifetime as the GCR flux is moderated by the solar cycle. However, the contribution from SEP ions varies on the order of hours and days and can exceed 10^4 counts per second during a large SEP event. Real 16–20 keV electrons from the solar wind superhalo [e.g., *Vocks*

Table 1. SEP Events Used in This Study

SEP Risetime	CME Shock Time	Number of Data Points Used	Max Background Count Rate (s^{-1})
9 Nov 2000, 19:27	12 Nov 2000, 11:20	503	1301
15 Apr 2001, 15:40	15 Apr 2001, 21:08	554	330
24 Sep 2001, 15:30	25 Sep 2001, 20:08	2207	2139
4 Nov 2001, 17:35	5 Nov 2001, 07:00	441	3521
23 Nov 2001, 02:00	24 Nov 2001, 08:00	2909	1021
29 Dec 2001, 02:00	29 Dec 2001, 07:40	241	117
9 Jan 2002, 00:00	11 Jan 2002, 07:10	2688	2272
16 Jul 2002, 18:00	19 Jul 2002, 22:21	647	2985
28 Oct 2003, 12:00	30 Oct 2003, 04:35	3250	10,420

et al., 2005], because of the small geometric factor, typically cause no counts during quiet periods, but electrons with these energies can be generated in large quantities when an interplanetary disturbance such as a CME (coronal mass ejection) shock sweeps past Mars, and can contribute substantially to the count rate at these times. Figure 4a in section 4 illustrates the various contributions to this count rate. Therefore, this count rate, which we refer to as the "background" count rate throughout the paper, is a useful proxy for SEP ions during a solar event but must be interpreted carefully. These issues are also discussed by *Brain et al.* [2012] and in substantial detail by G. T. Delory et al. (Energetic particles detected by the Electron Reflectometer instrument on the Mars Global Surveyor, 1999–2006, submitted to *Journal of Geophysical Research*, 2012) to which the interested reader is referred.

3. Data Analysis Methods

[9] Solar particle events can differ greatly in terms of the relative times of arrival of the fast solar energetic particles (SEPs) versus those that arrive with the lower-energy plasma and magnetic field disturbance indicative of a coronal mass ejection (CME) [*Jian et al.*, 2006; *Cane and Richardson*, 2003]. For each major solar particle event considered (see Table 1), we attempted to isolate the effects of the SEPs from the CME by considering only data obtained beginning with the initial rise in penetrating particle flux in the ER instrument but before the arrival of the CME-shock (this is identified by a sudden spike in real high-energy electron flux and magnetic field magnitude) [*Brain et al.*, 2012]. We combined this SEP time data from nine of the clearest solar particle events (from November 2000 to the famous "Halloween" events of 2003) with 20 days of MAG/ER data from an extremely quiet solar period in March 2004 to use as a control. This resulted in a data set of electron pitch angle distributions (PADs) collected in a range of different SEP flux environments, from very quiet to extremely intense.

[10] To isolate those distributions in which the electrons traveling upward and away from Mars originate in the collisional atmosphere, we restrict ourselves to PADs that display a clear loss cone, indicating that the MGS was magnetically connected to the collisional atmosphere [e.g., *Lillis et al.*, 2008a; *Brain et al.*, 2007], and in which the magnetic field makes an angle of at least 45° with respect to the local horizontal.

[11] There are three primary complications we must account for in identifying electrons traveling upward along magnetic field lines from the Martian atmosphere as having been produced by SEP impact ionization. The first is the instrumental background caused by penetrating particle radiation (i.e., SEPs directly striking the MCP of the Electron Reflectometer, as discussed earlier). During SEP events, we find that this source of instrumental "noise" (despite being useful for characterizing SEP flux) dominates the signal from the real electrons for energies above ~650 eV (at which electron fluxes are too low) and below 100 eV (at which a permanent attenuator reduces counts from real electrons by a factor of 50 to give the ER instrument a wider dynamic range). Therefore, we must restrict our analysis to just four electron energy channels, centered on 116, 191, 314, and 515 eV.

[12] The second complication is that converging magnetic field lines in the vicinity of magnetized regions of the Martian crust cause magnetic reflection of downward traveling electrons, forming a source of upward electron flux. We eliminate this issue by excluding all electron data collected in geographic regions where the crustal magnetic field magnitude at 185 km is >4 nT, according to the crustal magnetic field map of *Lillis et al.* [2008b], reducing to ~28,000 the number of valid PADs. This restriction to very weak crustal magnetic field regions, coupled with the requirement for clear loss cones and magnetic elevation angles greater than 45°, means that the overwhelming majority (~97%) of the valid PADs are on the nightside. This is because the draped magnetic field (which is characteristic of the Mars-solar wind interaction) [*Crider et al.*, 2004] is mostly tangential to the Martian surface on the dayside, while forming an approximately sunward-antisunward magnetotail that is mostly radial to the surface on the nightside. Therefore, to simplify matters, we keep only the nightside data. Figure 2 shows a magnetic map of Mars with the locations of every data point during our nine SEP events, as well as a histogram of the background count rates recorded at these points.

[13] The third complication is that collisions of regular, non-SEP-related downward traveling superthermal electrons with neutrals cause a substantial fraction of those electrons to be backscattered upward out of the atmosphere, forming another source of upward electron flux that is not related to the SEP ions. To account for this, we first calculate, as a function of energy, the distribution of the ratio of upward traveling to downward traveling electron fluxes over the nonmagnetic regions during only the quiet periods of low or nonexistent SEP ion fluxes (i.e., times when the background count rate is $<30\ s^{-1}$). Such distributions are shown in Figure 3 for our four electron energies. We then multiply the total downward traveling electron flux for every PAD by the median value of this up-down ratio (for each energy) in order to best estimate the upward traveling electron flux that is due only to the backscatter of the downward traveling superthermal electron flux and not due to the SEP ions. For every PAD, we then subtract this estimate of the backscattered flux from the actual measured upward traveling flux. We call the result the "residual" upward electron flux. It is this residual flux that is our best estimate for the

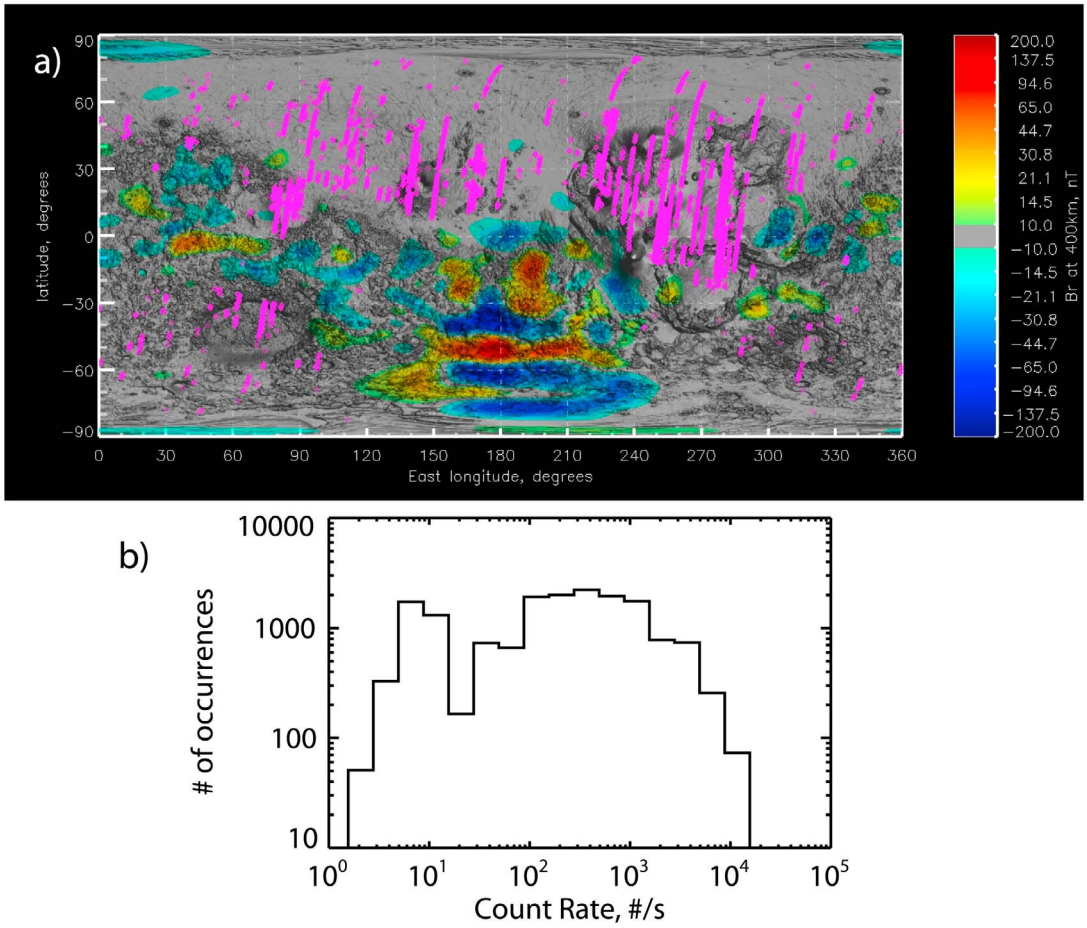

Figure 2. (a) Locations of the data points used in this study, plotted over on a map of radial crustal magnetic field measured at 400 km altitude [*Acuña et al.*, 2001]. (b) A histogram of the background count rates used in this study, spanning more than 4 orders of magnitude, from extremely quiet solar conditions to intense fluxes of SEP ions penetrating the ER instrument.

superthermal electrons that have been produced by SEP-impact ionization.

4. Case Study: Electron Pitch Angle Distributions During the 2003 Halloween Solar Event

[14] Works on the October–November 2003 Halloween series of solar disturbances (comprising large EUV-X-ray flares, interplanetary coronal mass ejections (ICMEs), and SEP events) and their effects on the terrestrial ionosphere-magnetosphere have been widely published [e.g., *Tsurutani et al.*, 2006]. At Mars, a series of magnetic and particle disturbances were observed over the course of ∼12 days [*Crider et al.*, 2005], with the largest SEP event and ICME seen at Mars starting on 28 October and continuing until 1 November [*Brain et al.*, 2012]. Figure 4a shows a time series of the aforementioned highest-energy channel count rate, which contains contributions from both penetrating SEP ions and real 16–20 keV electrons. The different colors in Figure 4 represent different SEP-related times: (1) pink refers to the quiet time before the disturbances began, (2) green represents the rapid rise in SEP ions, (3) red represents the ∼18 h during which there is an extremely high flux of SEP ions impacting the Martian atmosphere before the CME shock, (4) orange represents the time after the CME shock struck Mars, when both high-energy electrons and penetrating ions are present in the data, and (5) blue represents the time after the bulk of the event has occurred, during which there is only one small SEP ion event.

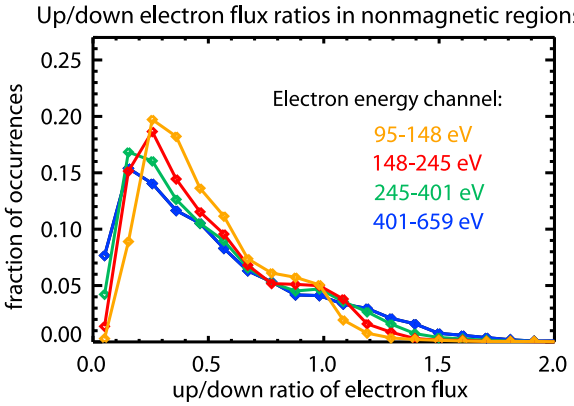

Figure 3. Histograms of the ratio of upward versus downward traveling electron fluxes in the nonmagnetic regions of the Martian nightside during extremely quiet solar periods.

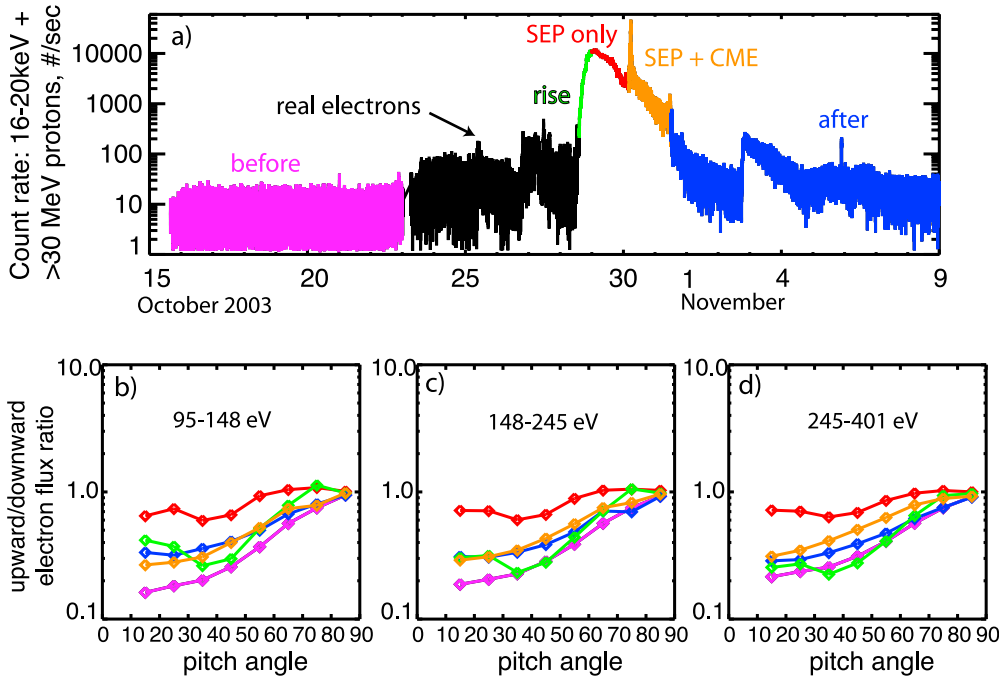

Figure 4. (a) A time series plot of background count rates before, during, and after the 2003 Halloween event, with different time intervals identified by color (see text). (b–d) The upward flux of superthermal electrons as a function of pitch angle (ϕ), normalized by the corresponding downward flux at a pitch angle of ($180° - \phi$), measured at 400 km altitude for three reliable energy channels for each of the color-coded time intervals.

[15] Figures 4b–4d shows the upward flux of superthermal electrons as a function of pitch angle (call it ϕ), normalized by the corresponding downward flux at a pitch angle of ($180° - \phi$), measured at 400 km altitude for three reliable energy channels for each of the aforementioned time intervals during the Halloween event. These up-down ratios are typically higher near 90° because downward traveling electrons with pitch angles closer to 90° backscatter from the atmosphere more easily than those with pitch angles closer to 0° [*Lillis et al.*, 2008a]. Through ionization of neutrals, we expect precipitating SEP ions to produce superthermal electrons, some of which should travel upward and be detected at spacecraft altitude (~400 km), so this ratio is expected to increase with increasing SEP ion-produced atmospheric ionization near and above the exobase (~150–200 km altitude). Several other factors can affect the shapes of these curves, including electrostatic potential differences, neutral density variations, and wave-particle scattering between the spacecraft and the exobase. Nonetheless, it is clear for these energies that these ratio curves are lowest before any of the disturbances begin (pink) and are highest during the time of greatest SEP flux (red), while they are broadly comparable during the SEP rise, postshock time, and immediate postevent times.

5. Statistical Study and Modeling

[16] Figure 5 shows how the residual electron flux from 95 to 659 eV varies with background count rate over our data set. We have split the data into five count rate ranges. As can be seen by the histogram shapes in Figure 5a, the residual flux of 245–401 eV electrons shows no departure from zero for count rates below 100; then it shows a small positive departure from count rates between 100 and ~2500, and a significant residual upward traveling electron flux for count rates above that. A similar pattern can be seen in Figures 5b and 5c, which show the median values of residual electron flux for each of the four energy channels for the same five count rate ranges, with linear and logarithmic ordinate axes, respectively. There appears to be a "step" in residual superthermal electron production past a certain penetrating ion flux level. This step may have physical significance or could simply be an artifact of small numbers of SEP events and different effective SEP geometric factors for each event. We do not wish to speculate either way. However, the trend of higher residual fluxes for higher background count rates is clear.

[17] This trend can be naïvely explained in the following manner. In the absence of direct measurements, we assume that the background count rate (i.e., a proxy for >30 MeV ions) of particles penetrating the ER instrument is itself a rough proxy for SEP ions of all energies above a few tens of keV (i.e., those that are not deflected by Mars' induced magnetosphere) [*Leblanc et al.*, 2002]. Those with energies below a few MeV deposit their energy at typical ionospheric altitudes of >90 km. As mentioned earlier, much of this deposited energy will go into ionization, increasing electron density throughout the ionosphere, with most electrons produced below ~150 km quickly thermalizing through collisions with neutrals [e.g., *Schunk and Nagy*, 2000]. SEP ion-induced electron production decreases exponentially with increasing altitude as the neutral density decreases, but for the highest SEP ion fluxes (the background count rates for which are above ~1000 s^{-1}), it appears that a sufficient

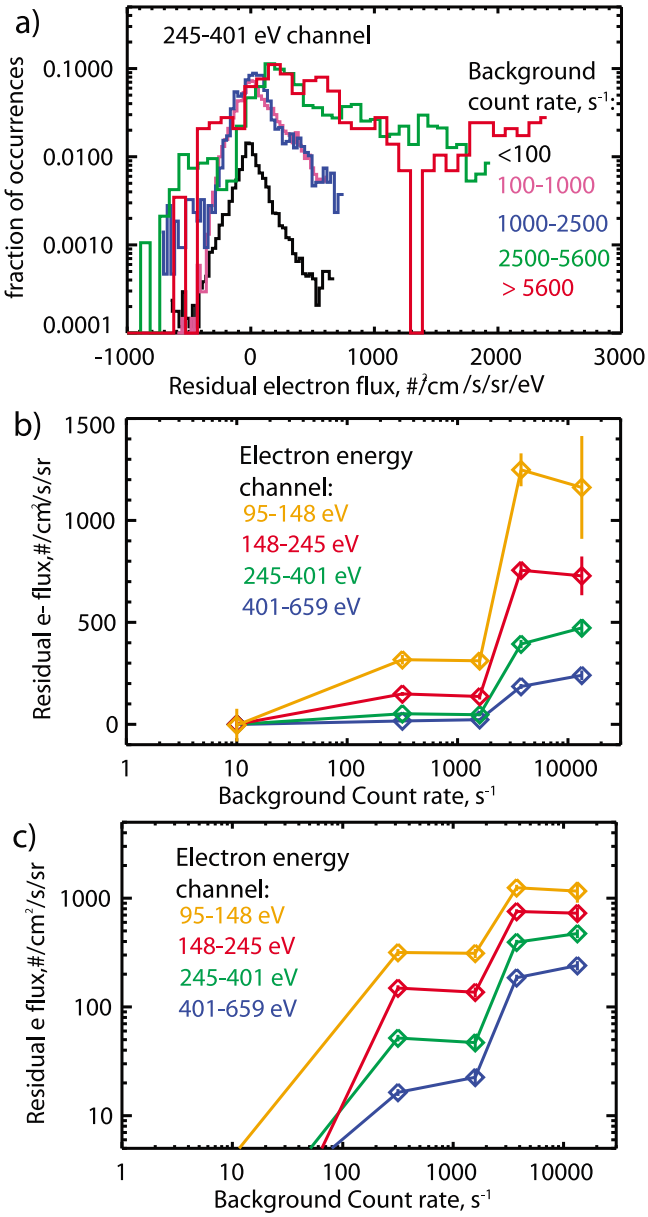

Figure 5. (a) Histograms of residual electron fluxes measured in the 245–401 eV energy channel for five different ranges of background count rate. (b, c) Median values of residual electron fluxes for each of the four reliable energy channels for the same five count rate ranges, with linear and logarithmic ordinate axes, respectively.

flux of >100 eV electrons are produced by ionization at high-enough altitudes (i.e., above which they can escape the atmosphere without thermalizing) that they are detectable as residual upward traveling electron fluxes in the ER instrument at 400 km. We also note that energetic SEPs can also enter the atmosphere at a high inclination angle and so deposit their energy at somewhat higher altitudes compared with vertical incidence.

[18] Ideally, we would use a comprehensive Monte Carlo energetic ion precipitation model to investigate whether the measured residual upward flux of electrons derived for the highest SEP ion fluxes could be reasonably produced by the fluxes of SEP ions known to have occurred following the 28 October 2003 X17 solar flare. Such a model would calculate secondary electron production rates and (importantly) model the transport of these electrons as they scatter with atmospheric neutrals and cause further ionization. The PLANETOCOSMICS GEANT4 framework can model energetic particle transport in planetary atmospheres, but is optimized for high-energy applications (e.g., cosmic rays) and is untrustworthy below a few keV [*Desorgher et al.*, 2006]. Therefore, there exists no appropriate publicly available model. Indeed, no such model exists in the published literature. In the absence of a comprehensive model and in the interest of keeping this paper focused on observations, we performed the following rough calculation of upward traveling secondary electron fluxes. The SEPs at Mars persisted for ~18 h before the arrival of the CME shock, so we consider only proton energies above 50 keV, whose transit times from the Sun to Mars were shorter than this interval (energies below this level are also significantly deflected by the magnetic pileup region of the Mars-solar wind interaction) [*Leblanc et al.*, 2002]. Since we have no proton measurements at Mars for this time, we take as a proxy the peak SEP proton spectrum measured on 29 October 2003, 05:59, by the Electron, Proton and Alpha Monitor (EPAM) instrument on the ACE spacecraft at ~1 AU [e.g., *Chiu et al.*, 1998]. This is a reasonable assumption since Mars and Earth were at almost the same Parker spiral magnetic field line during these events [*Crider et al.*, 2005]. The EPAM spectrum is shown in Figure 6a and goes up to ~3.5 MeV. We do not consider higher energies primarily because the lower fluxes at those energies should contribute comparatively a negligible amount to the production of electrons at altitudes (>~150 km) where those electrons can escape the atmosphere. We do not attempt to correct for the heliocentric distance between 1 and 1.4 AU since we do not know how beamed this SEP event was and because this is a plausibility study, not a rigorous quantitative comparison.

[19] While total proton impact ionization cross sections are available for the main Martian upper atmospheric constituents, atomic oxygen (O) and carbon dioxide (CO_2), differential cross sections for these species as functions of both primary proton and secondary electron energies are unavailable in the literature to the best of our knowledge. Therefore, as an approximation, differential cross sections for proton impact on helium [*Rudd*, 1988] were used and normalized such that the total cross sections (i.e., integrated over all ejected electron energies) matched the total proton impact ionization cross sections available for CO_2 and 0.5 times those values for molecular oxygen (O_2), taken from the review paper by *Rudd et al.* [1985]. Such cross sections for the ejection of electrons at our four reliable electron energies (~100–500 eV) are displayed in Figure 6b and show an extremely rapid falloff for incident proton energies below a certain cutoff energy: ~80, 130, 200, and 300 keV for 116, 190, 313, and 515 eV electrons, respectively.

[20] Differential production rates (in cm^{-3} s^{-1} eV^{-1}) for electrons of these energies were then calculated by integrating the product of the SEP flux and cross sections over the SEP energy range and multiplying by atmospheric number density, separately for both O and CO_2, which were then summed and multiplied by the 2π sr of solid angle from which the SEP flux comes. Neutral number densities are

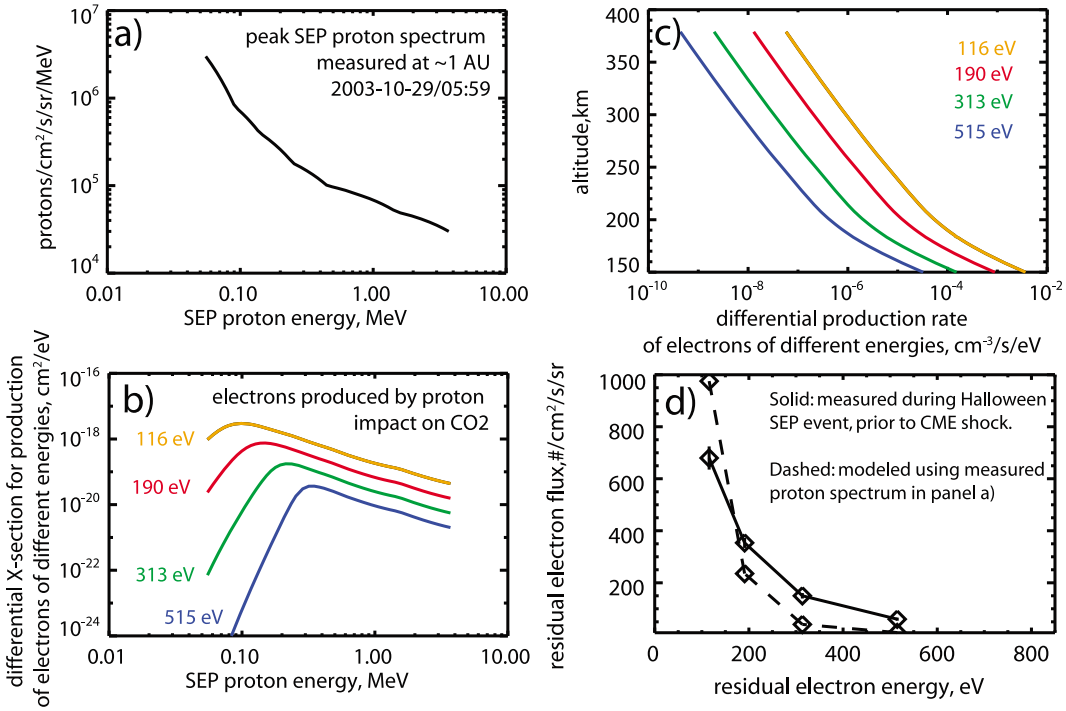

Figure 6. (a) SEP proton energy spectrum measured by the EPAM instrument on the ACE as spacecraft at ~1 AU. (b) Differential cross sections for production of 116, 190, 313, and 515 eV electrons by proton impact on CO_2 as a function of proton impact energy. (c) Calculated differential production rates of 116, 190, 313, and 515 eV electrons as functions of altitude. (d) The solid line represents residual upward traveling electron fluxes measured during the main SEP phase of the 2003 Halloween event, prior to the arrival of the CME shock, when the background count rates were between 1,500 and 10,000 s^{-1}.

taken from a standard equatorial equinox model reference atmosphere at 2 A.M. local time (same as the MGS Sun-synchronous orbit) from the Mars Climate Database [*Millour et al.*, 2008]. Only altitudes above 145 km were considered because the dimensionless scattering depth for superthermal electrons in this energy range becomes rapidly greater than unity for lower altitudes, i.e., electrons produced below this altitude have an extremely low probability of escaping the atmosphere [*Lillis et al.*, 2008a]. These production rates are shown in Figure 6c. Approximate fluxes (i.e., $cm^{-2}\ s^{-1}\ sr^{-1}\ eV^{-1}$) of such electrons detectable at the MGS orbital altitude of ~400 km were then calculated by integrating these production rates over all altitudes above 145 km and dividing by 2π. The resulting calculated residual upward electron fluxes are plotted as a function of energy in Figure 6d and compared with the average residual upward flux measured during the main SEP phase of the 2003 Halloween event, prior to the arrival of the CME shock (see Figure 4), when the background count rates were between 1400 and 10,000 s^{-1}.

[21] The substantial discrepancy between the measured and calculated upward traveling superthermal electrons fluxes can be attributed to the following factors:

1. The SEP spectrum used for the calculation was taken at 1 AU at a single moment in time in contrast to the many hours over which the preshock SEP event lasted at ~1.40 AU at Mars. This could easily result in factors of several differences in the actual precipitating SEP flux versus the calculation.

2. Electron ejection properties for proton impact on helium (as was assumed) may be substantially different than for O or CO_2.

3. The complex effects of elastic scattering-atmospheric backscatter of electrons in the Martian upper thermosphere have been ignored in this calculation and replaced with the very simple assumption that all electrons produced above 145 km can propagate upward and escape the atmosphere.

[22] Nonetheless, the observed and calculated values of SEP-produced electron fluxes are of a similar shape and certainly of the same order. Thus, it seems reasonable to assume that this "extra" upward traveling flux of superthermal electrons measured during the highest SEP flux events is due to substantial ionization of upper atmospheric neutrals caused by the precipitating SEPs. SEPs are certain to also produce, through primary and secondary ionization, electrons from thermal energies up to our data-imposed low-energy cutoff of 100 eV, making a significant contribution to ionospheric density.

6. SEP Ionization in the Context of Martian Aeronomy

[23] We would like to place SEP ionization in the broader context of Martian aeronomy and atmospheric escape. SEPs form an important ionization source in the Martian upper atmosphere, alongside photoionization and electron impact ionization (meteoritic and cosmic ray ionization are significant only below the homopause and therefore do not directly

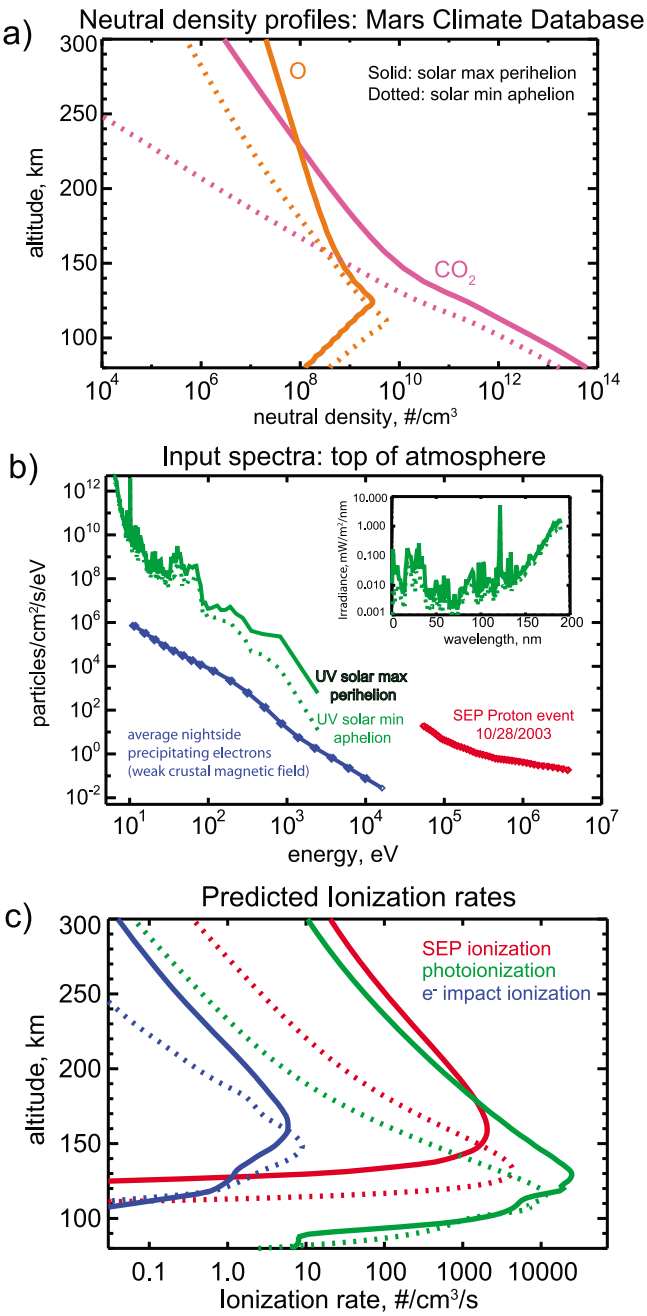

Figure 7. (a) Longitudinally averaged equatorial neutral density profiles of CO_2 (pink) and O (orange) from the Mars Climate Database [*Millour et al.*, 2008] corresponding to solar max-perihelion (solid lines) and solar min-aphelion conditions (dotted lines). (b) Energy spectra of energetic protons from the Halloween 2003 SEP event (red), average nightside precipitating electrons measured by MAG/ER away from magnetic cusp regions (blue), and solar UV at solar max-perihelion (green solid) and solar min-aphelion (dark green dotted). (c) Calculated ionization rates that are due to the particle spectra shown in Figure 7b precipitating into the neutral profiles shown in Figure 7a. Once again, solid means solar max-perihelion and dotted means solar min-aphelion.

impact atmospheric escape). A useful exercise in this regard is to directly compare roughly computed ionization profiles from three sources: SEPs, superthermal electron precipitation, and solar UV flux. We consider two representative equatorial, longitude-averaged, noon atmospheres from the Mars Climate Database [*Millour et al.*, 2008] that bracket conditions at Mars over the course of the solar cycle and of Mars' eccentric orbit: solar maximum perihelion and solar minimum aphelion. These are shown in Figure 7a. As the input spectra, we consider (1) the aforementioned SEP spectrum measured at the peak of the Halloween storm by ACE/EPAM, (2) the average nightside spectrum of downward traveling electrons as measured by MAG/ER from May 1999 until November 2006 in a 30° × 30° region of the Tharsis province devoid of magnetic cusps [*Lillis et al.*, 2011], and (3) approximately solar max-perihelion and solar min-aphelion solar UV spectra measured by the TIMED-SEE instrument at 1 AU, measured on 14 February 2002, Mars solar longitude Ls = 325°, and on 30 May 2008, Mars Ls = 78°, scaled and phase shifted to Mars [*Woods and Eparvier*, 2006]. These spectra are shown in Figure 7b.

[24] Photoionization rates were calculated using appropriate equations from *Schunk and Nagy* [2000, equations 9.17 and 9.26] and standard photoabsorption and photoionization cross sections of CO_2 and atomic oxygen from *Avakyan et al.* [1998], including photoelectron impact ionization by the method/parameterization of *Mendillo et al.* [2011]. Direct electron impact ionization rates were calculated using the MarMCET code framework [*Lillis et al.*, 2009]. SEP ionization rates were calculated (in the aforementioned absence of a comprehensive ion precipitation model) using a simple optical depth approach [*Schunk and Nagy*, 2000, equation 9.26], cross sections from *Rudd et al.* [1985], and assuming energies per electron-ion pair of 28 and 26 eV for CO_2 and O, respectively [*Wedlund et al.*, 2011]. This optical depth calculation may slightly overestimate the altitude of the ionization peak since it assumes all ionization from each proton happens at the same altitude, a fairly reasonable assumption since protons in matter deposit most of their energy at the end of their trajectory [*Ziegler et al.*, 2008]). Figure 7c shows the resulting ionization rate profiles, and Table 2 gives the total column-integrated ionization rates (units of cm^{-2} s^{-1}) for each of the six cases.

[25] We see that ionization rates from large SEP events such as the 2003 Halloween event approach, but do not exceed (photoionization + photoelectron impact ionization),

Table 2. Column-Integrated Ionization Rates (cm^{-2} s^{-1}) Due to SEP-Impact Ionization, Photoionization, and Electron-Impact Ionization

Ionization Source	Mars Climate Database Neutral Atmosphere Profile[a]	
	Solar Max-Perihelion	Solar Min-Aphelion
Peak SEP spectrum from 2003 Halloween event	1.10×10^{10}	1.10×10^{10}
Solar max-perihelion UV	8.03×10^{10}	NA
Solar min-aphelion UV	NA	2.53×10^{10}
Average precipitating nightside electron spectrum	9.61×10^{6}	8.51×10^{6}

[a]The Mars Climate Database is from the work of *Millour et al.* [2008].

rates at Mars, depending on season and solar cycle. SEP ionization easily dwarfs average nightside electron impact ionization (by 3 orders of magnitude). Although infrequently observed accelerated electron spectra [e.g., *Brain et al.*, 2006] can increase electron impact ionization locally by almost 2 orders of magnitude [*Lillis et al.*, 2011], such events are geographically isolated to small magnetic cusp regions, whereas SEP ionization is planetwide during an SEP event. As can be expected, peak altitudes are higher (by ~20 km) for the warmer solar max-perihelion atmosphere compared with the colder solar min-aphelion atmosphere. Since equilibrium electron density varies as the square root of the ionization rate, the difference between average electron-impact-induced electron densities and large-event SEP ionization-induced electron densities is 1–1.5 orders of magnitude.

[26] One important consequence of SEP ionization is that nightside wind-driven currents and electrojets will be much stronger than during quiet solar times. This should be especially true in regions of strong crustal magnetic fields, where the ionospheric dynamo region (i.e., the altitude range where the ions are collisionally controlled by the neutrals but the electrons are magnetized) should host a rich and complex pattern of currents corresponding to the magnetic topology of the superposition of the induced magnetotail and the highly inhomogeneous crustal fields.

[27] SEP ionization will also play an important role in atmospheric escape since ionization of atmospheric neutrals is the first step in pickup ion escape [*Fang et al.*, 2008], ion bulk escape [*Brace et al.*, 1987], and ion outflow [*Ergun et al.*, 2006]. SEP ionization plays a substantial role during an SEP event in increasing the "reservoir" of the ions available for escape. This is important because a CME shock often arrives after the peak of the primary SEPs have passed, bringing with it more locally shock-accelerated SEPs [e.g., *Ng et al.*, 2003] and turbulent magnetic conditions that can last for several days [*Crider et al.*, 2005], triggering wave-heating of ions and plasma instabilities that can lead to increased atmospheric escape [*Ergun et al.*, 2006]. Thus, the increased ionization caused by SEP precipitation into the atmosphere can "prime the system" for greatly increased atmospheric escape by an order of magnitude or more, as observed during an SEP event in 2006 and reported by *Futaana et al.* [2008]. Such "multiplier" mechanisms, whereby solar events cause atmospheric escape to increase by more than just the increase in ionization over the perennial dayside photoionization, will need to be fully taken into account when attempting to extrapolate backward in time to estimate the total integrated Martian escape to space over the history of the solar system.

7. Looking Forward

[28] The kind of approximate analysis in this paper is the best we can hope to achieve with such limited data and modeling tools. To properly diagnose the effects of SEP precipitation, we will need nearly simultaneous measurements of (1) SEP energy spectra and anisotropy above and within the atmosphere, (2) thermospheric ion, electron, and neutral temperatures and densities, and (3) fluxes of SEP-produced electrons and ions (with composition) escaping from the atmosphere. The 2013 MAVEN Mars Scout mission [*Jakosky*, 2011], with its comprehensive suite of particles, fields, and remote sensing instrumentation, promises to provide the necessary measurements to far better characterize and understand solar energetic particle precipitation and its effects on the Martian atmosphere, including the SEP-produced electrons analyzed in this paper. In addition, the Mars Science Laboratory Radiation Assessment Detector (RAD) instrument will be on the Martian surface starting in mid-2012, measuring ions from 2 to 100 MeV/nucleon [*Wimmer-Schweingruber et al.*, 2011], providing further information on the SEP spectrum and how it is modulated by the planet, the atmosphere, and the subsurface.

[29] **Acknowledgments.** R. J. Lillis' work on this paper was supported by the NASA Mars Data Analysis Program, grant NNX11AI87G, and the Mars Fundamental Research Program, grant NNX09AD43G. R. P. Lin was supported in part by the WCU grant (R31–10016) funded by the Korean Ministry of Education, Science, and Technology.

References

Acuña, M. H., et al. (2001), Magnetic field of Mars: Summary of results from the aerobraking and mapping orbits, *J. Geophys. Res.*, *106*, 23,403–23,417, doi:10.1029/2000JE001404.

Albee, A. L., R. E. Arvidson, F. Palluconi, and T. Thorpe (2001), Overview of the Mars Global Surveyor mission, *J. Geophys. Res.*, *106*, 23,291–23,316, doi:10.1029/2000JE001306.

Avakyan, S. V., R. N. Il'in, V. M. Lavrov, and G. N. Ogurtsov (1998), *Collision Processes and Excitation of the Ultraviolet Emission from Planetary Atmospheric Gases: A Handbook of Cross Sections*, Gordon and Breach, London.

Bibring, J. P., et al. (2006), Global mineralogical and aqueous Mars history derived from OMEGA/Mars Express data, *Science*, *312*, 400–404, doi:10.1126/science.1122659.

Brace, L. H., W. T. Kasprzak, H. A. Taylor, R. F. Theis, C. T. Russell, A. Barnes, J. D. Mihalov, and D. M. Hunten (1987), The ionotail of Venus: Its configuration and evidence for ion escape, *J. Geophys. Res.*, *92*(A1), 15–26, doi:10.1029/JA092iA01p00015.

Brain, D. A., J. S. Halekas, L. M. Peticolas, R. P. Lin, J. G. Luhmann, D. L. Mitchell, G. T. Delory, S. W. Bougher, M. H. Acuña, and H. Rème (2006), On the origin of aurorae on Mars, *Geophys. Res. Lett.*, *33*, L01201, doi:10.1029/2005GL024782.

Brain, D. A., R. J. Lillis, D. L. Mitchell, J. S. Halekas, and R. P. Lin (2007), Electron pitch angle distributions as indicators of magnetic field topology near Mars, *J. Geophys. Res.*, *112*, A09201, doi:10.1029/2007JA012435.

Brain, D. A., G. T. Delory, R. J. Lillis, D. Ulusen, D. L. Mitchell, and J. G. Luhmann (2012), MGS measurements of solar storms and their effects, in *The Energetic Particle Radiation Hazard en Route to and at Mars*, edited by S. McKenna-Lawlor, Int. Acad. of Astronaut., Paris, in press.

Cane, H. V., and I. G. Richardson (2003), Interplanetary coronal mass ejections in the near-Earth solar wind during 1996–2002, *J. Geophys. Res.*, *108*(A4), 1156, doi:10.1029/2002JA009817.

Chevalier, M. W., W. B. Peter, U. S. Inan, T. F. Bell, and M. Spasojevic (2007), Remote sensing of ionospheric disturbances associated with energetic particle precipitation using the South Pole VLF beacon, *J. Geophys. Res.*, *112*, A11306, doi:10.1029/2007JA012425.

Chiu, M. C., et al. (1998), ACE spacecraft, *Space Sci. Rev.*, *86*, 257–284, doi:10.1023/A:1005002013459.

Crider, D. H., D. A. Brain, M. H. Acuña, D. Vignes, C. Mazelle, and C. Bertucci (2004), Mars Global Surveyor observations of solar wind magnetic field draping around Mars, *Space Sci. Rev.*, *111*, 203–221, doi:10.1023/B:SPAC.0000032714.66124.4e.

Crider, D. H., J. Espley, D. A. Brain, D. L. Mitchell, J. E. P. Connerney, and M. H. Acuña (2005), Mars Global Surveyor observations of the Halloween 2003 solar superstorm's encounter with Mars, *J. Geophys. Res.*, *110*, A09S21, doi:10.1029/2004JA010881.

Desorgher, L., E. O. Fluckiger, and M. Gurtner (2006), The PLANETOCOSMICS Geant4 application, in *Proceedings of the 36th COSPAR Scientific Assembly*, vol. 36, p. 2361, Comm. on Space Res., Paris.

Dmitriev, A. V., and H.-C. Yeh (2008), Geomagnetic signatures of sudden ionospheric disturbances during extreme solar radiation events, *J. Atmos. Sol. Terr. Phys.*, *70*, 1971–1984, doi:10.1016/j.jastp.2008.05.008.

Ergun, R. E., L. Andersson, W. K. Peterson, D. Brain, G. T. Delory, D. L. Mitchell, R. P. Lin, and A. W. Yau (2006), Role of plasma waves in

Mars' atmospheric loss, *Geophys. Res. Lett.*, *33*, L14103, doi:10.1029/2006GL025785.

Espley, J. R., W. M. Farrell, D. A. Brain, D. D. Morgan, B. Cantor, J. J. Plaut, M. H. Acuña, and G. Picardi (2007), Absorption of MARSIS radar signals: Solar energetic particles and the daytime ionosphere, *Geophys. Res. Lett.*, *34*, L09101, doi:10.1029/2006GL028829.

Fang, X., M. W. Liemohn, A. F. Nagy, Y. Ma, D. L. De Zeeuw, J. U. Kozyra, and T. H. Zurbuchen (2008), Pickup oxygen ion velocity space and spatial distribution around Mars, *J. Geophys. Res.*, *113*, A02210, doi:10.1029/2007JA012736.

Ferguson, B. B., J. C. Cain, D. H. Crider, D. A. Brain, and E. M. Harnett (2005), External fields on the nightside of Mars at Mars Global Surveyor mapping altitudes, *Geophys. Res. Lett.*, *32*, L16105, doi:10.1029/2004GL021964.

Futaana, Y., et al. (2008), Mars Express and Venus Express multi-point observations of geoeffective solar flare events in December 2006, *Planet. Space Sci.*, *56*, 873–880, doi:10.1016/j.pss.2007.10.014.

Galand, M., D. Lummerzheim, A. W. Stephan, B. C. Bush, and S. Chakrabarti (2002), Electron and proton aurora observed spectroscopically in the far ultraviolet, *J. Geophys. Res.*, *107*(A7), 1129, doi:10.1029/2001JA000235.

Jackman, C. H., et al. (2008), Short- and medium-term atmospheric constituent effects of very large solar proton events, *Atmos. Chem. Phys.*, *8*, 765–785, doi:10.5194/acp-8-765-2008.

Jakosky, B. M. (2011), The 2013 Mars Atmosphere and Volatile EvolutioN (MAVEN) Mission to Mars, paper presented at The Fourth International Workshop on the Mars Atmosphere: Modelling and Observations, Lab. de Meteorol. Dyn., Paris, 8–11 February.

Jian, L., C. T. Russell, J. G. Luhmann, and R. M. Skoug (2006), Properties of interplanetary coronal mass ejections at one AU During 1995–2004, *Solar Phys.*, *239*, 393–436.

Leblanc, F., J. G. Luhmann, R. E. Johnson, and E. Chassefiere (2002), Some expected impacts of a solar energetic particle event at Mars, *J. Geophys. Res.*, *107*(A5), 1058, doi:10.1029/2001JA900178.

Lillis, R. J., D. L. Mitchell, R. P. Lin, and M. H. Acuña (2008a), Electron reflectometry in the Martian atmosphere, *Icarus*, *194*, 544–561, doi:10.1016/j.icarus.2007.09.030.

Lillis, R. J., H. V. Frey, M. Manga, D. L. Mitchell, R. P. Lin, M. H. Acuña, and S. W. Bougher (2008b), An improved crustal magnetic field map of Mars from electron reflectometry: Highland volcano magmatic history and the end of the Martian dynamo, *Icarus*, *194*, 575–596, doi:10.1016/j.icarus.2007.09.032.

Lillis, R. J., M. O. Fillingim, L. M. Peticolas, D. A. Brain, R. P. Lin, and S. W. Bougher (2009), Nightside ionosphere of Mars: Modeling the effects of crustal magnetic fields and electron pitch angle distributions on electron impact ionization, *J. Geophys. Res.*, *114*, E11009, doi:10.1029/2009JE003379.

Lillis, R. J., D. A. Brain, S. L. England, P. Withers, M. O. Fillingim, and A. Safaeinili (2010), Total electron content in the Mars ionosphere: Temporal studies and dependence on solar EUV flux, *J. Geophys. Res.*, *115*, A11314, doi:10.1029/2010JA015698.

Lillis, R. J., M. O. Fillingim, and D. A. Brain (2011), Three-dimensional structure of the Martian nightside ionosphere: Predicted rates of impact ionization from Mars Global Surveyor MAG/ER measurements of precipitating electrons, *J. Geophys. Res.*, *116*, A12317, doi:10.1029/2011JA016982.

Luhmann, J. G., C. Zeitlin, R. Turner, D. A. Brain, G. Delory, J. G. Lyon, and W. Boynton (2007), Solar energetic particles in near-Mars space, *J. Geophys. Res.*, *112*, E10001, doi:10.1029/2006JE002886.

Lummerzheim, D., M. Galand, and M. Kubota (2003), Optical emissions from proton aurora, *Sodankylä Geophys. Obs. Publ.*, *92*, 1–5.

Mendillo, M., A. Lollo, P. Withers, M. Matta, M. Pätzold, and S. Tellmann (2011), Modeling Mars' ionosphere with constraints from same-day observations by Mars Global Surveyor and Mars Express, *J. Geophys. Res.*, *116*, A11303, doi:10.1029/2011JA016865.

Millour, E., et al. (2008), The latest (version 4.3) Mars climate database, *LPI Contrib.*, *1447*, 9029.

Mitchell, D. L., R. P. Lin, C. Mazelle, H. Rème, P. A. Cloutier, J. E. P. Connerney, M. H. Acuna, and N. F. Ness (2001), Probing Mars' crustal magnetic field and ionosphere with the MGS Electron Reflectometer, *J. Geophys. Res.*, *106*(E10), 23,419–23,427, doi:10.1029/2000JE001435.

Mitra, A. P., and J. N. Rowe (1974), Ionospheric constraints of mesospheric nitric oxide, *J. Atmos. Terr. Phys.*, *36*, 1797–1808.

Moore, T. E., and J. L. Horwitz (2007), Stellar ablation of planetary atmospheres, *Rev. Geophys.*, *45*, RG3002, doi:10.1029/2005RG000194.

Morgan, D. D., D. A. Gurnett, D. L. Kirchner, R. L. Huff, D. A. Brain, W. V. Boynton, M. H. Acuña, J. J. Plaut, and G. Picardi (2006), Solar control of radar wave absorption by the Martian ionosphere, *Geophys. Res. Lett.*, *33*, L13202, doi:10.1029/2006GL026637.

Ng, C. K., D. V. Reames, and A. J. Tylka (2003), Modeling shock-accelerated solar energetic particles coupled to interplanetary Alfvén waves, *Astrophys. J.*, *591*, 461–485, doi:10.1086/375293.

Reagan, J. B., and T. M. Watt (1976), Simultaneous satellite and radar studies of the *D* region ionosphere during the intense solar particle events of August 1972, *J. Geophys. Res.*, *81*(25), 4579–4596, doi:10.1029/JA081i025p04579.

Reames, D. V., C. K. Ng, and D. Berdichevsky (2001), Angular distributions of solar energetic particles, *Astrophys. J.*, *550*, 1064–1074, doi:10.1086/319810.

Rudd, M. E. (1988), Differential cross sections for secondary electron production by proton impact, *Phys. Rev. A*, *38*, 6129–6137, doi:10.1103/PhysRevA.38.6129.

Rudd, M. E., Y.-K. Kim, D. H. Madison, and J. W. Gallagher (1985), Electron production in proton collisions: Total cross sections, *Rev. Mod. Phys.*, *57*, 965–994, doi:10.1103/RevModPhys.57.965.

Schunk, R. W., and A. F. Nagy (2000), *Ionospheres: Physics, Plasma Physics, and Chemistry*, Cambridge Univ. Press, New York, doi:10.1017/CBO9780511551772.

Seppälä, A., M. A. Clilverd, C. J. Rodger, P. T. Verronen, and E. Turunen (2008), The effects of hard-spectra solar proton events on the middle atmosphere, *J. Geophys. Res.*, *113*, A11311, doi:10.1029/2008JA013517.

Solomon, S., G. C. Reid, D. W. Rusch, and R. J. Thomas (1983), Mesospheric ozone depletion during the solar proton event of July 13, 1982: 2. Comparison between theory and measurement, *Geophys. Res. Lett.*, *10*, 257, doi:10.1029/GL010i004p00257.

Tsurutani, B. T., A. J. Mannucci, B. Iijima, F. L. Guarnieri, W. D. Gonzalez, D. L. Judge, P. Gangopadhyay, and J. Pap (2006), The extreme Halloween 2003 solar flares (and Bastille Day, 2000 Flare), ICMEs, and resultant extreme ionospheric effects: A review, *Adv. Space Res.*, *37*, 1583–1588, doi:10.1016/j.asr.2005.05.114.

Velinov, P. (1968), On ionization in the ionospheric *D*-region by galactic and solar cosmic rays, *J. Atmos. Terr. Phys.*, *30*, 1891–1905, doi:10.1016/0021-9169(68)90031-7.

Velinov, P. I. Y., L. N. Mateev, and C. W. Spassov (1996), An improved model for the influence of cosmic rays and high energy particles on the ionosphere and middle atmosphere, *Adv. Space Res.*, *18*(3), 23–27, doi: 10.1016/0273-1177(95)00831-X.

Vocks, C., C. Salem, R. P. Lin, and G. Mann (2005), Electron halo and Strahl formation in the solar wind by resonant interaction with whistler waves, *Astron. J.*, *627*, 540–549.

Wedlund, C. S., G. Gronoff, J. Lilensten, H. Menager, and M. Barthelemy (2011), Comprehensive calculation of the energy per ion pair or *W* values for five major planetary upper atmospheres, *Ann. Geophys.*, *29*, 187–195, doi:10.5194/angeo-29-187-2011.

Wimmer-Schweingruber, R. F., C. Martin, E. Boehm, S. Boettcher, A. Kharytonov, J. Koehler, M. Kuhnke, B. Ehresmann, D. M. Hasler, and C. Zeitlin (2011), Measuring neutrons and gamma rays on Mars, The Mars Science Laboratory Radiation Assessment Detector MSL/RAD, *Lunar Planet. Sci.*, *XLII*, Abstract 1793.

Woods, T. N., and F. G. Eparvier (2006), Solar ultraviolet variability during the TIMED mission, *Adv. Space Res.*, *37*, 219–224, doi:10.1016/j.asr.2004.10.006.

Zadorozhnyi, A. M., V. N. Kikhtenko, G. A. Kokin, O. M. Raspopov, O. V. Shumilov, G. A. Tuchkov, M. I. Tyasto, A. F. Chizhov, and O. V. Shtyrkov (1992), Response of the middle atmosphere to solar proton events in October 1989, *Geomagn. Aeron.*, *32*, 32–40.

Ziegler, J. F., J. P. Biersack and M. D. Ziegler (2008), *The Stopping and Range of Ions in Solids*, Lulu Press, Morrisville, N. C.

D. A. Brain, Laboratory for Atmospheric and Space Physics, University of Colorado, 1234 Innovation Dr., Boulder, CO 80303, USA.

G. T. Delory, R. J. Lillis, R. P. Lin, J. G. Luhmann, and D. L. Mitchell, Space Sciences Laboratory, University of California Berkeley, 7 Gauss Way, Berkeley, CA 94720, USA. (rlillis@ssl.berkeley.edu)